Dimerization of Electrochemically Generated Radical Ions under High Pressure

Vladimir Mazine and Jürgen Heinze*

Institut für Physikalische Chemie, Universität Freiburg, Albertstrasse 21, Freiburg i.Br. D-79104, Germany

Received: August 13, 2003; In Final Form: October 23, 2003

For the first time, organic electrochemical processes in aprotic media were studied by means of cyclic voltammetry at pressures of up to 300 MPa. The measurements at different concentrations, scan rates, temperatures, and pressures provide evidence of the reversible dimerization of electrochemically generated radical anions of trinitrotoluene, naphthalenedicarbonitrile, 9-cyanoanthracene, and radical cations of triphenylamine. The reaction volumes of the dimerization of the substances studied were determined as −36, −19, −35, and −23 $cm^3\ mol^{-1}$, respectively. Their negative values manifest the shift of the equilibrium of the dimerization under high pressure toward the formation of dimers. The small difference between the respective reaction volumes in acetonitrile and dichloromethane points to the dominance of the intrinsic geometry changes over solvation effects in this process.

1. Introduction

In the last two decades, several research groups have used UV/vis or ESR-spectroscopy as well as electrochemical methods to show that radical anions of acceptor-substituted aromatics may dimerize despite their electrostatic repulsion.[1−12] In aprotic media, this dimerization process may be reversible in that the reoxidation of the dimer produces the initial monomer. The reduction behavior of 9-cyanoanthracene (**1**) has been intensively discussed. Parker et al.[1−3] and Savéant et al.[4−6] have shown that after reduction **1** dimerizes at the 10-position of the anthracene moiety, forming a σ-dimer. However, the mechanism of dimerization has remained controversial. Reaction paths discussed involve inter alia radical−substrate or radical−radical couplings as key dimerization steps. In most cases, the first variant has been ruled out after a thorough analysis of the kinetic data.[5] For the second variant, Hammerich and Parker[1,3] postulated a two-step mechanism (Scheme 1) to explain the comparatively slow kinetics of the process; however, the existence of the intermediate π-dimer has not been proved experimentally.

SCHEME 1: Two-Step Radical−Radical Dimerization

$$2M \overset{+2e}{\rightleftharpoons} 2M^{\bullet -} \rightleftharpoons [M\cdots M]^{2-} \rightleftharpoons D^{2+}$$

Savéant et al.[4,5] in turn suggested a direct one-step radical−radical dimerization and proposed that steric factors should be responsible for the slow kinetics. Later on Savéant improved this concept and pointed out that a significant decrease of entropy can accompany the formation of the transition state because of the increase of solvation resulting from the localization of negative charges of reacting particles, thus slowing down the dimerization rate.[6] In addition, the estimates of Savéant demonstrated that the enthalpy of electrostatic repulsion between the two 9-cyanoanthracene moieties is compensated by increased solvation in the transition state leading to a small activation enthalpy. Thermodynamic considerations revealed that the energy of strong electrostatic repulsion can be only compensated by the enthalpy of formation of a σ-bond and by no means by that of a π-bond. This led to the concept of radical−radical coupling with the formation of σ-dimer as a key step in the mechanism of 9-cyanoanthracene electrodimerization.

A subsequent development is the introduction of a diffusion controlled radical−radical coupling mechanism for 9-cyanoanthracene and other cyano-substituted derivatives of anthracene and naphthalene.

SCHEME 2: Reductive and Oxidative Electrodimerization

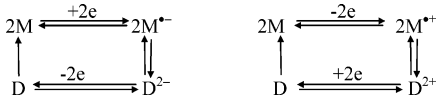

Heinze et al.[7] showed that the dependence of the dimerization rate constant on the value of dielectric constant of the reaction medium follows the Debye−Smoluchowski theory of diffusion-controlled reactions of charged species.[13] According to this theory, the kinetics of dimerization of charged particles are strongly dependent on the value of the dielectric constant (ϵ) of the solvent. In equally charged particles, the repulsive forces in solvent with high dielectric constants should be low.

Equations 1−3 give the expression for the rate constant k_{2d} of the reaction between two charged particles A and B with charge numbers Z_A and Z_B:

$$k_{2d} = 4\pi \times 10^{-3} N_A{}^2 (D_A + D_B) R_{AB} \Phi_{AB} \tag{1}$$

$$\Phi_{AB} = \frac{\varphi}{e^{\varphi} - 1} \tag{2}$$

$$\varphi = \frac{Z_A Z_B e^2}{R_{AB} \epsilon kT} \tag{3}$$

where R_{AB} is the sum of van der Waals radii of particles A and B. One can see that the rate constant decreases with the decrease of ϵ. Thus, in polar reaction media the electrostatic repulsion of equally charged radical ions can be shielded to a great extent providing a low activation enthalpy and making the dimerization reaction diffusion controlled. This assumption is strongly

* Address correspondence to this author. Tel.: +49-761-203-6202; fax: +49-761-203-6237; e-mail: juergen.heinze@physchem.uni-freiburg.de.

10.1021/jp0364147 CCC: $27.50
Published on Web 12/10/2003

supported by experimental data for dimerization of cyano-substituted derivatives of anthracene and naphthalene in different media.[7]

A similar mechanism has been postulated for the reversible dimerization of radical cations generated during the anodic oxidation of diphenylpolyenes[8] and methylated bithiophenes.[9] Spectroscopic studies have established analogous processes for aromatic amines, substituted olefins, and tetrathiofulvalene.[10,11] Heinze et al.[12] have shown that 1,3,5-tripyrrolidinobenzene having been electrochemically oxidized also follows this mechanism of σ-dimer formation, which after reduction "reversibly" dissociates generating the monomer species. One-step and two-step mechanisms of dimerization in this case are not distinguishable by means of electrochemical kinetics analysis, and our present work is based on the assumption that the one-step mechanism is valid for the chosen model compounds.

The mechanism of reversible electrodimerization is important and in principle cannot be excluded in any process dealing with radical ions, though the kinetics of the overall process is strongly dependent upon the chemical structure of radical ions as well as upon the properties of the reaction medium. The corresponding equilibrium and rate constants may vary by several orders of magnitude simply because of changing of the solvent.[7] Thus, in many cases, ignoring this mechanism can hamper the correct interpretation of the experimental data. For example, this concerns annihilation reaction of radical cations and anions where the corresponding rate constant may be drastically reduced by simultaneous individual dimerization reactions of cations or anions.[14]

Performing the electrochemical experiment under high pressure in the 10^8 Pa range affects the equilibrium of the dimerization stage and, thus, gives direct insight into the mechanism of electrodimerization and related processes.

The pressure dependence of the thermodynamic equilibrium constant of a reaction is usually represented in terms of the volume of reaction.[15] For the reaction of two particles A and B:

$$A + B \rightleftarrows AB$$

the reaction volume

$$\Delta\bar{V} = \bar{V}_{AB} - \bar{V}_A - \bar{V}_B \tag{4}$$

where $\bar{V}_{AB}$, $\bar{V}_A$, $\bar{V}_B$ are the corresponding molar volumes.

From the pressure dependence of the chemical potential of the substance in the ideal solution

$$\left(\frac{\partial \mu_i}{\partial P}\right)_T = \bar{V}_i \tag{5}$$

we can determine the relationship between the equilibrium constant of the reaction K and the reaction volume

$$(\partial \ln K/\partial P)_T = -\Delta\bar{V}/RT \tag{6}$$

Transition-state theory gives the analogous relationship for the rate constant of the reaction:

$$(\partial \ln k_f/\partial P)_T = -\Delta\bar{V}^*/RT \tag{7}$$

where

$$\Delta\bar{V}^* = \bar{V}_{A-B}^* - \bar{V}_A - \bar{V}_B \tag{8}$$

is activation volume of the reaction and $\bar{V}_{A-B}^*$ is molar volume of the transition complex.

Figure 1. A photograph of the high-pressure experimental setup.

In diluted solutions, the partial molar volume of dissolved species is determined mostly by two factors: the intrinsic geometry of molecules roughly expressed with van der Waals radii and the interaction of the species with the molecules of solvent causing electrostriction.[14] Thus, in the first approximation the reaction volume can be considered as a sum of two components:

$$\Delta\bar{V} = \bar{V}_{intr} + \bar{V}_{solv} \tag{9}$$

The intrinsic reaction volume corresponds to geometry changes in the reactants, and the solvation reaction volume originates from the electrostriction effects and thus, it is essentially dependent upon the polarity of the reaction medium.

The literature on high-pressure electrochemistry is very extensive, although only a few research groups conduct studies in the range of hundreds of MPa. Swaddle et al. have studied the electron-transfer reactions of the complex ions of iron and cobalt and long-range electron-transfer reactions in proteins in aqueous solutions[16−19] and in acetonitrile[20] under pressures up to 250 MPa. Tregloan et al. have used cyclic staircase voltammetry to study redox reaction volumes of metal complexes under the pressures up to 120 MPa in water and acetonitrile.[21−23] Exceptionally high pressures of 1 GPa have been achieved by Faulkner et al. in their studies of the solvation and thermodynamics of inorganic electron-transfer reactions in aqueous media.[24,25] Although numerous studies of organic electrochemical processes in near-critical and supercritical fluids have been performed, the pressures have not been high enough to deliver the information about reaction volumes.

Thus, to the best of our knowledge, this is the first high-pressure electrochemical study of pure organic compound in aprotic media.

2. Experimental and Simulations

The general view of the high-pressure experimental setup is presented in Figure 1. The high pressure of up to 400 Mpa was

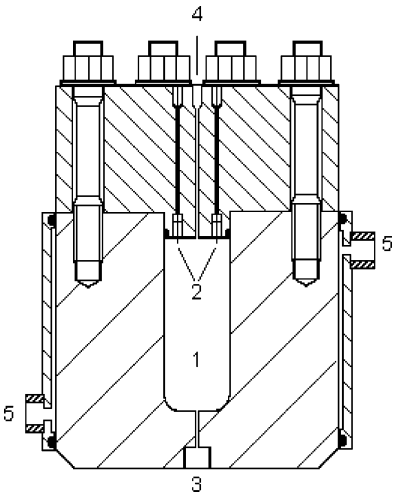

Figure 2. Drawing of the high-pressure compartment; working volume (1); current connectors (2); high-pressure junction (3); gas-release vent (4); inlet and outlet of water jacket (5).

generated with the help of a specially designed multistep pressure intensifier (New Ways of Analytics, 79540 Lörrach). The intensifier had two pneumatic and two hydraulic steps. The first step was fed by compressed air at 1 MPa; heptane was used as the hydraulic medium.

The working compartment presented schematically in Figure 2 was connected on top of the intensifier by means of standard high-pressure junction and was easily mounted and dismounted. The working compartment was supplied with four current connectors and a water jacket for temperature control and had a cylindrical working volume 90 mm high and 30 mm in diameter that permitted it to house an electrochemical cell of the appropriate size. The stability and performance of the high-pressure compartment was assured by the proper choice of the materials for the manufacture of the body and the current connectors.[26]

The electrochemical cell for high-pressure experiments must have variable volume to translate the pressure from the hydraulic medium to the electrolyte solution and to compensate the density change of the solvent under high pressure[27] and, on the other hand, it must reliably isolate the solution under study from the hydraulic medium. An additional difficulty in aprotic solvents is the fact that most of the synthetic materials that could be used for sealing the cell swell in acetonitrile and dichloromethane. Under high-pressure, swelling becomes even more pronounced, deforming Teflon parts and destroying glass parts of the cell. After testing several models of the cell, stainless steel was chosen as the material for the main parts.

The cell (Figure 3) consisted of two coaxial stainless steel cylinders sealed by two Kalrez O-rings. The inner cylinder had a standard screw for a Shott cap with a ring spacer for inserting a soft-glass tube with two Pt wires soldered in it. The face of one wire (0.5 or 0.2 mm diameter) served as a working electrode; the other wire was covered with silver and served as a quasi reference electrode. The inner cylinder served as an auxiliary electrode. Extra dry solvents (acetonitrile and dichloromethane) were prepared using conventional procedures, $TBAPF_6$ from Fluka was used as supporting electrolyte, a trinitrotoluene sample of HPLC-reference grade was kindly presented by Dynamite Nobel, and all other chemicals were purchased from Aldrich and used without further purification.

The working solutions were prepared in a glass cell. Residual water was removed by passing solutions through the built-in column with alumina. After performing the measurements at

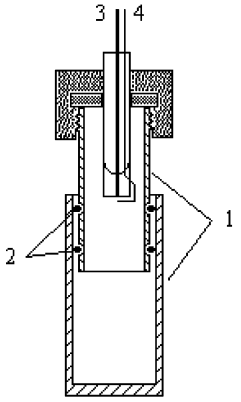

Figure 3. Electrochemical cell for high-pressure measurements; stainless steel cylinders, the inner serving as auxiliary electrode (1); Kalrez O-rings (2); working electrode (3); reference electrode (4).

normal pressure, a working solution was transferred to the high-pressure cell in the glovebox under argon. The electrochemical measurements were performed with a home-built potentiostat and a PAR Model 175 universal programmer.

CV data were collected for two to three concentrations of each substance. For the given conditions (temperature and pressure), a set of curves was measured with potential sweep rates varying from 0.01 to 100 V s^{-1}. Cyclic voltammograms that were simulated according to the given mechanism were fitted simultaneously to these data. All simulations were carried out with the help of DigiSim software version 3.03 capable of simulating two-electron-transfer reactions.

3. Results and Discussion

Four model substances were used in this study. Substances **1**, **2,** and **3** when being electrochemically reduced produce radical anions and substance **4** when being oxidized forms radical cations, all of which can reversibly dimerize.

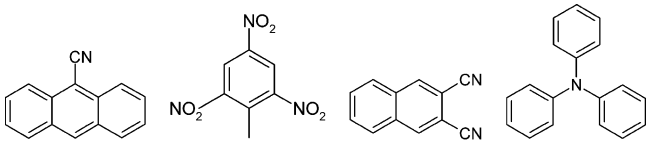

1 **2** **3** **4**

For all these substances, measurements performed under normal pressure evidenced behavior that corresponded with the reversible dimerization mechanism. Characteristic of this mechanism are one redox wave in the forward and reverse scans at relatively low sweep rates, indicating the "reversible" formation of radical ion. As the sweep rate increases, a second peak appears in the reverse scan at more positive (negative in radical cations formation) potential, the sign of the dimer; simultaneously, the "reversible" peak decreases. Further sweep rate increasing causes the dimer peak to diminish and the monomer peak to return back in its place (Figure 4).

CV data measured at different temperatures, concentrations, and sweep rates were successfully fitted with the curves simulated according to the mechanism. The fitting was performed until the simulated curves with the same kinetic parameters satisfied all the CV data measured under given conditions, including experiments with different potential scan rates and different concentrations of reactants (Figure 5).

The application of high pressure significantly shifts the equilibrium of the second step of the process (dimerization)

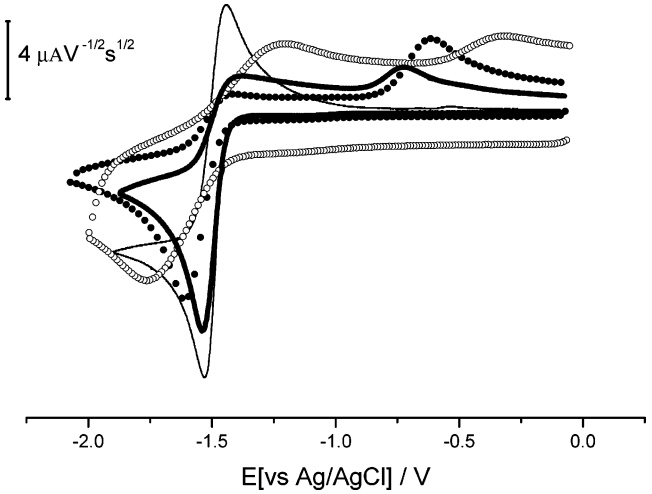

Figure 4. Normalized cyclic voltammograms ($=i/v^{1/2}$) for the reduction of 1 mM of **1** in acetonitrile/0.1 M $TBAPF_6$ solution under normal conditions; $v = 10$ mV s^{-1} (−), $v = 0.5$ V s^{-1} (—), $v = 10$ V s^{-1} (●), $v = 100$ V s^{-1} (○).

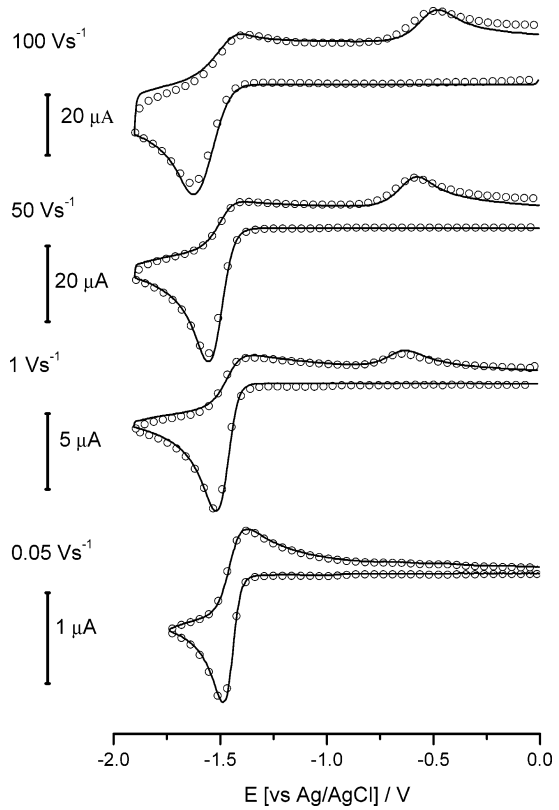

Figure 5. Experimental voltammograms (○) of **1** ($c = 1 \times 10^{-3}$ M, in acetonitrile/0.1 M $TBAPF_6$) and corresponding simulations (−) at different scan rates at room temperature ($T = 293$ K) and normal pressure; simulation parameters: $E_m^0 = -1.5$ V; $k_{s,m}^0 = 0.035$ cm s^{-1}; $\alpha_m = 0.5$; $E_d^0 = -0.68$ V; $k_{s,d}^0 = 0.021$ cm s^{-1}; $\alpha_d = 0.5$; $K_{dim} = 9.8 \times 10^4$ L mol^{-1}; $k_{dim,f} = 1.5 \times 10^6$ L mol^{-1} s^{-1}; $D_m = 8.5 \times 10^{-5}$ cm^2 s^{-1}; $D_d = 2.5 \times 10^{-5}$ cm^2 s^{-1}.

toward the formation of the dimer species. This effect manifests itself in the voltammograms as an increase in the ratio of the peak current at the potential of the dimer oxidation (reduction in **4**) to the peak current at the potential of the radical ion oxidation (reduction).

Figure 6 illustrates this effect in the voltammograms of the model substances.

Simulated curves also successfully fitted the high-pressure data (Figure 7).

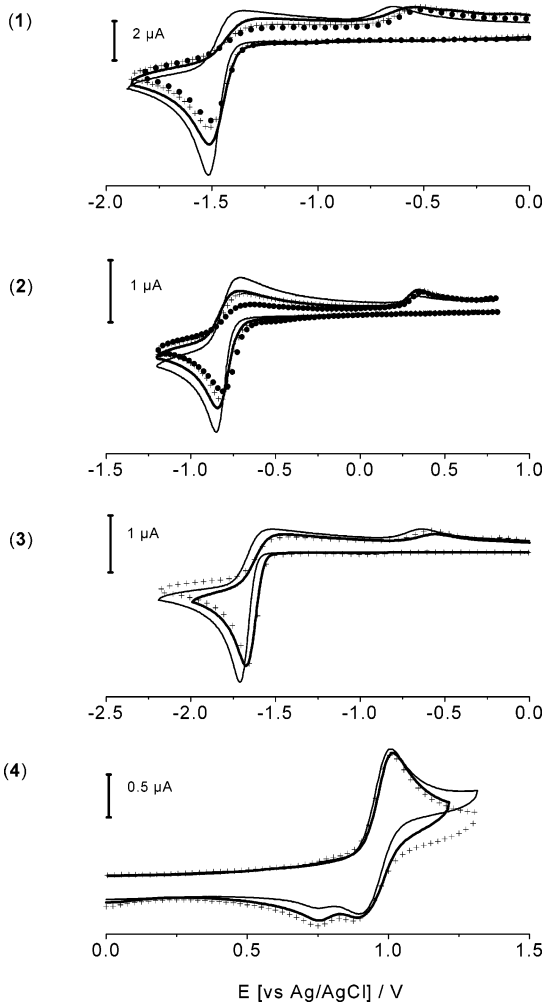

Figure 6. The effect of high pressure on the shape of cyclic voltammograms of model substances **1**−**4**; $c = 1 \times 10^{-3}$ M at normal pressure, in acetonitrile/0.1 M $TBAPF_6$; scan rate 1 V s^{-1}; normal pressure (−); 100 MPa (—); 200 MPa (+); 400 MPa (●).

TABLE 1: Standard Enthalpy, Standard Entropy, and Reaction Volume of the Dimerization Reaction of Studied Radical Ions in Acetonitrile

	$\Delta H°$/ kJ mol^{-1}	$\Delta S°$/ J mol^{-1} K^{-1}	ΔV/ cm^3 mol^{-1}
9-cyanoanthracene	−55.4	−89.1	−35
trinitrotoluene	−40.0	−49.8	−36
naphthalenedicarbonitrile	−47.4	−52.3	−19
triphenylamine	−41.1	−42.7	−23

This gives solid support to the proposed mechanism and allows determination of the thermodynamical parameters of the process by the linear least-squares procedure (Figure 8) using the equations

$$R \ln K = -\Delta H \times \frac{1}{T} + \Delta S$$

$$(\partial \ln K/\partial P)_T = -\Delta V/RT$$

Table 1 presents thermodynamical parameters determined in this way. In all cases, the enthalpy of dimerization is significantly less than the enthalpy of C−C bond formation. This is in keeping with the fact that, in these cases, two equally charged particles participate in the reaction and the electrostatic repulsion must be taken into account. The negative values of the entropy are characteristic of the dimerization processes. The negative

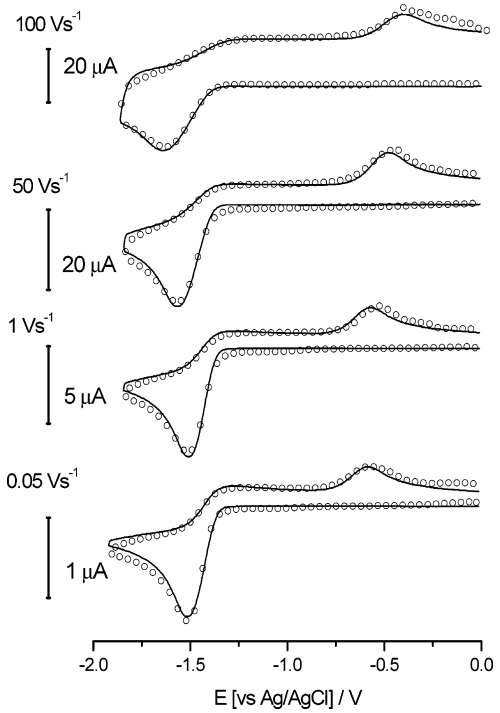

Figure 7. Experimental voltammograms (○) of **1** ($C = 1 \times 10^{-3}$ M, in acetonitrile/0.1 M $TBAPF_6$) and corresponding simulations (−) at different scan rates at room temperature ($T = 293$ K) and under pressure of 300 MPa; simulation parameters: $E_m^0 = -1.48$ V; $k_{s,m}^0 = 0.034$ cm s^{-1}; $\alpha_m = 0.5$; $E_d^0 = -0.67$ V; $k_{s,d}^0 = 0.019$ cm s^{-1}; $\alpha_{dim} = 0.5$; $K_{dim} = 1.4 \times 10^7$ L mol^{-1}; $k_{dim,f} = 9.5 \times 10^7$ L mol^{-1} s^{-1}; $D_m = 1.5 \times 10^{-5}$ cm^2 s^{-1}; $D_d = 3.5 \times 10^{-6}$ cm^2 s^{-1}.

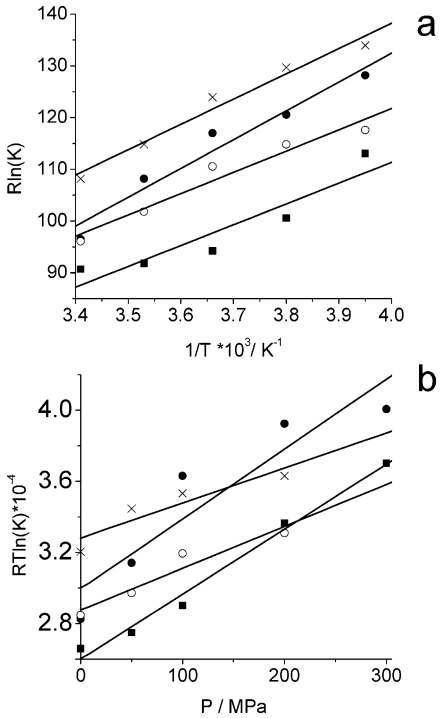

Figure 8. Determination of $\Delta H°$ and $\Delta S°$ (a), and ΔV (b) of the reaction of radical ions dimerization; substance **1** (●), substance **2** (■), substance **3** (×), substance **4** (○), the values of equilibrium constants for the dimerization were determined by fitting of experimental cyclic voltammograms with simulated ones; least-squares procedure results (−).

reaction volumes manifest the significant shift in the equilibrium of the dimerization step toward the formation of dimer species on account of the high pressure.

TABLE 2: Activation Parameters of the Dimerization Reaction

	activation volume $\Delta\bar{V}$*/cm^3 mol^{-1}	activation energy E_a/kJ mol^{-1}
9-cyanoanthracene	−33	8.9
trinitrotoluene	−25	6.1
naphthalenedicarbonitrile	−5.5	11.5
triphenylamine	−8.6	12.3

TABLE 3: Equilibrium Constants, Standard Enthalpy, Standard Entropy, and Reaction Volume of 9-Cyanoanthracene Radical Anions Dimerization in Acetonitrile and Dichloromethane

	CH_3CN	CH_2Cl_2
ϵ	37.5	8.9
K (normal pressure)	11×10^4	4.1×10^4
K (300 MPa)	14.0×10^6	2.5×10^6
$\Delta H°$/kJ mol^{-1}	55.5	31.2
$\Delta S°$/J mol^{-1} K^{-1}	−89	−21.3
ΔV/cm^3 mol^{-1}	−36	−32

The kinetics of the dimerization process is also influenced by the applied pressure. Activation volume values were determined for the model substances in accordance with eq 4. These data, along with activation energies determined from Arrhenius plots, are presented in Table 2. In all cases, activation volumes of the forward reactions have negative values, which signifies acceleration of the forward reaction as the pressure increases.

To estimate the relative significance of the intrinsic and solvation parts of the reaction volume for **1** we performed two series of experiments in acetonitrile and dichloromethane solutions. As shown previously,[7] the dimerization of radical anions of **1** is less favorable in less polar media. This can be seen from the values of the equilibrium constants at room temperature and enthalpy and entropy of the dimerization in these solvents (Table 3). On the contrary, there is not much difference between the reaction volumes for these two media. The difference lies within the margin of error of our measurements and calculations. Thus, at least in **1** the intrinsic geometry changes make the main contribution to the reaction volume. We can assume that this weak dependence of the reaction volume on the nature of the medium indicates also that there is no strong change in solvation during the reaction. That turns us back to the idea of a diffusion-controlled dimerization step. These experimental results are also in line with recent quantum mechanical calculations performed by Lacroix et al.[28] They have shown that in contrast to the situation in a vacuum, where the dimerization of radical cations is extremely unfavorable because of electrostatic repulsion, in polar solvents (water has been used for the calculations) the dimerization rate constant can be very close or even above that of a diffusion-controlled process. In this case, the significant reorganization of solvation atmosphere is hardly imaginable because of rather symmetrical structure of pyrrole radical cation, the dimerization of which has been studied in that paper.

4. Conclusion

For the first time, the high-pressure technique has been used to study organic electrochemical processes in aprotic media. Assuming the mechanism of reversible electrodimerization for the processes studied, we have shown that in 10^8 Pa pressure range the reaction volumes of the dimerization stage are negative, that is, the application of high pressure enhances the dimerization of electrochemically generated radical ions of studied substances.

Performing electrochemical experiments under high pressure provides new opportunities in mechanistic studies. For instance, we have shown that for 9-cyanoanthracene radical anion dimerization the intrinsic part plays a more important role than the solvation part in the overall reaction volume.

Acknowledgment. Financial support by the Volkswagen Foundation (Project No. I 75517-518) is gratefully acknowledged.

References and Notes

(1) Hammerich, O.; Parker, V. D. *Acta Chem. Scand.* **1981**, *B 35*, 341−347.

(2) Hammerich, O.; Parker, V. D. *Acta Chem. Scand.* **1983**, *B 37*, 851−856.

(3) Hammerich, O.; Parker, V. D. *Acta Chem. Scand.* **1983**, *B 37*, 379−392.

(4) Amatore, C.; Pinson, J.; Savéant, J. M. *J. Electroanal. Chem.* **1982**, *137*, 143−148.

(5) Savéant, J. M. *Acta Chem. Scand.* **1983**, *B 37*, 365−378.

(6) Savéant, J. M. *Acta Chem. Scand.* **1988**, *B 42*, 721−727.

(7) El-Desoky, H.; Heinze, J.; Ghoneim, M. M. *Electrochem. Commun.* **2001**, *3*, 697−702.

(8) Smie, A.; Heinze, J. *Angew. Chem., Int. Ed. Engl.* **1997**, *36*, 363−367.

(9) Tschuncky, P.; Heinze, J.; Smie, A.; Engelmann, G.; Kossmehl, G. *J. Electroanal. Chem.* **1997**, *433*, 223−226.

(10) Bäuerle, P.; Segelbacher, U.; Maier, A.; Mehring, M. *J. Am. Chem. Soc.* **1993**, *115*, 10217−10219.

(11) Bäuerle, P.; Segelbacher, U.; Gaudl, K.-U.; Huttenlocher, D.; Mehring, M. *Angew. Chem.* **1993**, *105*, 125−127; *Angew. Chem., Int. Ed. Engl.* **1993**, *32*, 76−78.

(12) Heinze, J.; Willmann, C.; Bäuerle, P. *Angew. Chem., Int. Ed.* **2001**, *40*, 2861−2864.

(13) Debye, P. *Trans. Electrochem. Soc.* **1942**, *82*, 265.

(14) Van Eldik, R.; Asano, T.; Le Noble, J. *Chem. Rev.* **1989**, *89*, 549−688.

(15) Kapturkiewicz, A. In *Advances in Electrochemical Science and Engineering*; Alkire, R., Gerischer, H., Kolb, D. M., Tobias, C. W., Eds.; Wiley-VCH: Weinheim, 1997; Vol. 5, Chapter 1, p 1.

(16) Sun, J.; Wishart, J. F.; van Eldik, R.; Shalders, R. D.; Swaddle, T. W. *J. Am. Chem. Soc.* **1995**, *117*, 2600−2605.

(17) Jolley, W. H.; Stranks, D. R.; Swaddle, T. W. *Inorg. Chem.* **1990**, *29*, 385−389.

(18) Doine, H.; Whitcombe, T. W.; Swaddle, T. W. *Can. J. Chem.* **1992**, *70*, 81−88.

(19) Takagi, H.; Swaddle, T. W. *Inorg. Chem.* **1992**, *31*, 4669−4673.

(20) Doine, H.; Swaddle, T. W. *Can. J. Chem.* **1988**, *66*, 2763−2767.

(21) Sachinidis, J.; Shalders, R. D.; Tregloan, P. A. *J. Electroanal. Chem.* **1992**, *327*, 219−234.

(22) Sachinidis, J.; Shalders, R. D.; Tregloan, P. A. *Inorg. Chem.* **1994**, *33*, 6180−6186.

(23) Sachinidis, J.; Shalders, R. D.; Tregloan, P. A. *Inorg. Chem.* **1996**, *35*, 2497−2503.

(24) Golas, J.; Drickamer, H. G.; Faulkner, L. R. *J. Phys. Chem.* **1991**, *95*, 10191−10197.

(25) Cruañes, M. T.; Drickamer, H. G.; Faulkner, L. R. *J. Phys. Chem.* **1992**, *96*, 9888−9892.

(26) Swaddle, T. S. In *High-pressure Techniques in Chemistry and Physics. A Practical Approach*; Holzapfel, W. B., Isaacs, N. S., Eds.; Oxford, 1997; Chapter 7.3, p 343.

(27) Francesconi, A. Z.; Franck, E. U.; Lentz, H. *Ber. Bunsen-Ges. Phys. Chem.* **1975**, *79*, 897−901.

(28) Lacroix, J.-C.; Maurel, F.; Lacaze, P.-C. *J. Am. Chem. Soc.* **2000**, *123*, 1989−1996.